Bioconjugate Chemistry

Article

pubs.acs.org/bc

Fluorophore:Dendrimer Ratio Impacts Cellular Uptake and Intracellular Fluorescence Lifetime

Casey A. Dougherty,[†] Sriram Vaidyanathan,[‡] Bradford G. Orr,[§] and Mark M. Banaszak Holl*[,†,‡]

[†]Department of Chemistry, [‡]Department of Biomedical Engineering, and [§]Department of Physics, University of Michigan, Ann Arbor, Michigan 48109, United States

Supporting Information

ABSTRACT: G5-NH_2-$TAMRA_n$ (n = 1−4, 5+, and 1.5_{avg}) were prepared with n = 1−4 as a precise dye:dendrimer ratio, 5+ as a mixture of dendrimers with 5 or more dye per dendrimer, and 1.5_{avg} as a Poisson distribution of dye:dendrimer ratios with a mean of 1.5 dye per dendrimer. The absorption intensity increased sublinearly with n whereas the fluorescence emission and lifetime decreased with an increasing number of dyes per dendrimer. Flow cytometry was employed to quantify uptake into HEK293A cells. Dendrimers with 2−4 dyes were found to have greater uptake than dendrimer with a single dye. Fluorescence lifetime imaging microscopy (FLIM) showed that the different dye:dendrimer ratio alone was sufficient to change the fluorescence lifetime of the material observed inside cells. We also observed that the lifetime of G5-NH_2-$TAMRA_{5+}$ increased when present in the cell as compared to solution. However, cells treated with G5-NH_2-$TAMRA_{1.5avg}$ did not exhibit the high lifetime components present in G5-NH_2-$TAMRA_1$ and G5-NH_2-$TAMRA_{5+}$. In general, the effects of the dye:dendrimer ratio on fluorescence lifetime were of similar magnitude to environmentally induced lifetime shifts.

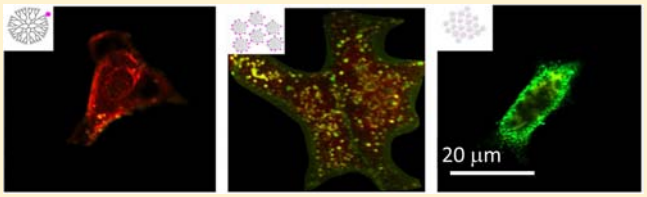

INTRODUCTION

Cationic polymers are employed for a variety of biological applications involving transport of the polymer into cells including transfection agents for oligonucleotides, antibacterial agents, and drug delivery agents.[1−5] In order to probe the uptake and cellular localization properties, the polymer is often modified with fluorescent dye.[6] In this case, it is important to understand how the presence of dye modifies the behavior of the polymer. Such dye-modified polymers are also of interest as models for the biodistribution behavior of the polymer when it is modified with multiple hydrophobic moieties, such as targeting agents or drugs. Dye:polymer conjugates are often complex mixtures. Dye conjugated to a large excess of reactive sites on the polymer will result in a Poisson distribution of dye:polymer particle ratios that is superimposed on the molecular weight (MW) distribution of the base polymer.[7,8] Materials containing a large degree of dispersion in both MW and hydrophobicity per particle are expected to exhibit a range of biological uptake and distribution behavior.[9−12] An additional complication is the impact of dye conjugation: specifically, the impact that the localization of multiple dyes on a given polymer particle has on the photophysical properties of the dye. This high effective concentration of dye can result in substantial differences in both fluorescence intensity and lifetime per polymer particle.[6,13,14] Given the importance of dye-conjugates to probing the mechanisms of cationic polymers as antibacterial agents and as vectors for gene and drug delivery, we have explored the ways in which employing distributions of dye-conjugates impacts interpretations of cell uptake and localization for polycationic polymers.

The generation of systematically varied dye:polymer ratios for a cationic polymer is a challenging problem. Most commonly, a mean variation in dye:polymer ratio is achieved under stochastic reaction conditions that generate a statistical distribution of ratios and a mixture of hydrophobic and photophysical properties. The distribution of ratios is quite broad with substantial overlap of materials for different means, making comparisons between different conjugate averages difficult to interpret. Table 1 provides an illustrative example for the case of stochastic conjugates containing an average of 1−4 dyes for generation 5 poly(amidoamine) (G5 PAMAM) dendrimer. For these cases, the population of the mean percentage varies between about 1/5th and 1/3rd of the total material.

In order to prepare a set of cationic polymer samples containing a uniform dye:polymer ratio across all particles in the sample, it is necessary to decouple the number of dyes per particle from the particle MW. This is synthetically challenging since a large polymer particle will generally have more functional attachment sites, and therefore have a statistically greater chance of multiple dye conjugation. We achieved the decoupling of conjugation number from MW by separating a stochastic mixture of TAMRA dye conjugates based on the differential hydrophobicity imparted to each dendrimer particle by the presence of dye. In this study, we report the semipreparative reverse-phase high performance liquid chro-

Received: December 5, 2014
Revised: January 26, 2015
Published: January 27, 2015

DOI: 10.1021/bc5005735
Bioconjugate Chem. 2015, 26, 304−315

Table 1. Statistical Conjugation Heterogeneity for a G5 PAMAM (G5-dye$_n$) Containing 93 Arms and 1−4 Conjugated Dyes[a]

	percentage of each dye:dendrimer ratio										
Avg n	0	1	2	3	4	5	6	7	8	9	10
1	36.6	**37.0**	18.5	6.1	1.5	0.3	0.1	-	-	-	-
2	13.2	27.1	**27.4**	18.2	9.0	3.5	1.1	0.3	0.1	-	-
3	4.7	14.7	22.5	**22.8**	17.1	10.1	5.0	2.0	0.7	0.2	0.1
4	1.7	7.0	14.5	19.8	**20.0**	16.0	10.5	5.9	2.8	1.2	0.5

[a]For each value of n, the percentage for the mean value is highlighted in bold.

matography (rp-HPLC) fractionation of the stochastic mixture of dye:dendrimer ratios in G5-NH_2-$TAMRA_{1.5(avg)}$ into samples containing a single dye:dendrimer ratio (n = 1−4) as well as a sample containing n > 5: G5-NH_2-$TAMRA_n$ (n = 1−4, 5+). Characterization of the precise dye:dendrimer ratio fractions was carried out by analytical reverse-phase ultrahigh performance liquid chromatography (rp-UPLC), ^{1}H NMR spectroscopy, and MALDI-TOF mass spectrometry.

With this new set of precise ratio dye conjugates available, we tested the following implicit and explicit hypotheses that underlie previous literature studies employing mixtures containing stochastic distributions of dye:polymer ratios:

H1. Uptake of cationic polymers can be quantified by measuring the change in mean fluorescence of cells using flow cytometry.

H2. The components of a stochastic distribution of dye:polymer ratios have a similar collective trend in terms of environmental lifetime response, so the mixture can be used to probe internal cellular environments.

H3. The changes in environmentally based lifetime response are large as compared to difference in lifetime response associated with differences in dye:polymer ratio.

The three hypotheses were tested by measuring the uptake, fluorescence emission, and fluorescence lifetime of G5-NH_2-$TAMRA_n$ (n = 1−4, 5+, 1.5_{avg}) in HEK293A cells using flow cytometry, fluorimetry, and fluorescence lifetime imaging microscopy (FLIM). In addition, fluorescence emission and lifetime control experiments were performed in aqueous solutions with controlled pH, ionic strength, and biomolecule concentration to test the impacts of these conditions on the fluorescence properties. We show that, contrary to the expectations of H1, mean fluorescence is a poor measure for comparing the relative cellular uptake of differing dye:polymer ratios. FLIM studies of the dye-conjugates taken up into the HEK293A cells suggest that the fluorescence lifetime response to the cellular environment is very sensitive to the dye:polymer ratio, raising concerns about H2 and H3. These studies indicate caution should be exercised when interpreting FLIM data for stochastic dye mixtures in biological systems. Biological systems have the capacity for fractionating a sample,[9−12,15] much like an HPLC column, prior to the fluorescence measurement. For such a system, this study indicates that it is critical to know the dye:polymer ratio dependent properties of the material being measured in order to accurately compare fluorescence intensities or to make use of differences in fluorescence lifetime.

RESULTS AND DISCUSSION

The importance of cationic polymers for biological applications has led to a number of recent studies addressing the use of dye conjugates. Mier et al. studied the stochastic conjugation of multiple dyes including fluorescein, rhodamine, coumarin, and dansyl to PAMAM dendrimers.[16] With the exception of dansyl, they found that fluorescence intensity decreased as the mean number of dyes per dendrimer increased. The intensity decrease was attributed to a combination of a small Stokes shift leading to quenching and the high effective concentration that results from multiple dyes conjugated to the same polymer core. By way of contrast, in dansyl-modified PAMAM materials, fluorescence increased with increasing dye:dendrimer ratio, presumably due to the large Stokes shift of 195 nm. Schroeder et al. examined Cy3 and Cy5 dye optical properties conjugated to generation 5 (G5) PAMAM or G6 PAMAM dendrimer in order to create a new set of materials for biological imaging with enhanced stability and increased accuracy in single molecule imaging.[17] Dendrimer mixtures with an average of 8 Cy5 dyes gave slower photobleaching compared to free dye with a 6- to 10-fold increase in photobleaching lifetime value for the G5 PAMAM conjugates. The dendrimer conjugates with an average of 14 Cy5 dyes on G6 PAMAM showed a ∼17-fold increase in photobleaching lifetime value. The mean conjugation numbers employed in this case generate mixtures with <0.5% of the material having zero or one dye. This eliminates the most dramatic difference in effective local concentration and the related variation in photophysical properties that occurs when the dye:polymer ratio changes from 1 to 2. Wagner et al. employed stochastically prepared G3 PAMAM dendrimer conjugated to a mean of 1 Alexa Fluor 555 dye to quantify the rate constant of dendrimer uptake in Caplan-1 cells.[18] Interestingly, reverse-phase high performance liquid chromatography (rp-HPLC) did not resolve different species as being present in this case, although separation has been achieved for other dye ligands.[14] In this study, an effective mass transfer coefficient was determined for the mixture of dye:dendrimer ratios present in the sample. Many additional studies addressing the uptake of polycationic polymer−dye conjugates have been discussed in a series of comprehensive reviews.[6] These studies are of broad interest because the level of hydrophobicity is known to alter a polymer's ability to permeate cell membranes,[19] as well as impact transfection efficiency,[20−24] biodistribution,[15] and pharmokinetics.[25,26] Colocalization of polymer−fluorophore conjugates based on surface functionality[17,27] has also been shown. In all cases, the presence of broad conjugation heterogeneity in the stochastic mixtures of polymer−dye conjugates has prevented a detailed understanding of what fraction or fractions of the conjugates are providing the desired biological activity.

In order to focus this study on the impact of dye conjugation heterogeneity, it was necessary to employ a cationic polymer that contained a minimal MW distribution while remaining convenient for generating a systematic change in the dye:polymer ratio. In addition, the polymer MW must be large enough to accommodate a number of dyes and still maintain good water solubility for all dye:polymer ratios. We selected G5 PAMAM dendrimer as this material is readily available commercially, has excellent water solubility, and has a

DOI: 10.1021/bc5005735
Bioconjugate Chem. 2015, 26, 304−315

Scheme 1. . Synthesis, Isolation, and Characterization of G5-NH_2-TAMRA$_n$ (n = 0, 1, 2, 3, 4, 5+, 1.5$_{avg}$) Samples[a]

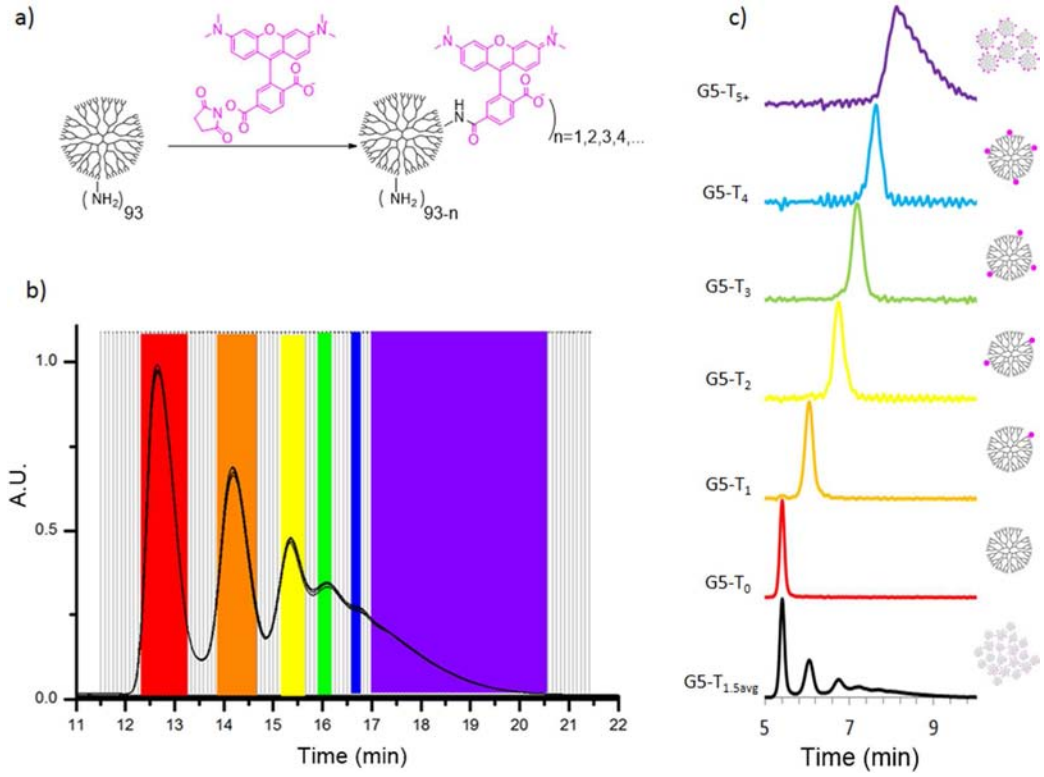

[a](a) Stochastic conjugation of TAMRA to G5 PAMAM dendrimer. (b) Isolation of G5-NH_2-TAMRA$_n$ employing semi-preparative rp-HPLC. (c) Reinjection of combined fractions on analytical rp-UPLC to determine purity. n = 1.5$_{avg}$ (black), 0 (red), 1 (orange), 2 (yellow), 3 (green), 4 (blue), and 5+ (purple).

sufficiently large MW (theoretically 28 826 Da) to maintain solubility upon conjugation with multiple dyes. In addition, we have developed rp-HPLC protocols that remove all of the trailing generations (G1−G4: 1430 to 14 215 Da MW) as well as the dimer, trimer, and tetramer oligomers (~50 000 to 120 000 Da range) typically present in G5 PAMAM dendrimer.[28] The purified G5 PAMAM material obtained from the rp-HPLC purification has an average of 93 primary amine terminal arms per particle (as compared to the theoretical 128 arms), a M_n of 25 130 Da, and a M_w of 27 140 Da (M_n/M_w = 1.08). The full mass range of the isolated monomer G5 PAMAM material was 21 000 to 30 000 Da.

Isolation and Characterization of Dendrimer−TAMRA Conjugates. Direct conjugation of TAMRA to G5 PAMAM dendrimer results in a Poisson distribution of dye:dendrimer ratios (Scheme 1a). The material was separated using semipreparative rp-HPLC (Scheme 1b) into fractions containing precise dye:dendrimer ratios (n = 1−4) as well as a sample where $n \geq 5$. The isolated fractions were reinjected into an analytical UPLC to determine purity (Scheme 1c) and further characterized using ^{1}H NMR spectroscopy, emission and absorption measurements, MALDI-TOF-MS, and fluorescence lifetime imaging microscopy (FLIM).

Analytical UPLC provides the most sensitive measure of the number of dyes present per dendrimer particle.[14] The shift resulting from the addition of each dye to the dendrimer scaffold for the first two dyes is substantially larger than the breadth of the peak resulting from the MW distribution of the G5 PAMAM dendrimer (Scheme 1c). As the number of dyes increases, the incremental value of the hydrophobicity induced shift decreases. The UPLC method detects the dye:dendrimer particle ratio induced shifts in the context of the full defect structure of the polymer, which generates the observed peak width.[14] The number of dyes measured for each fraction G5-NH_2-TAMRA$_n$ are n = 0.0, 1.0, 2.0, 3.0, and 4.0, and an average of 6.8 dye:dendrimer for the $n \geq 5$ fraction (Supporting Information Table S1). The average number of TAMRA dyes per dendrimer was also assessed using ^{1}H NMR spectroscopy by comparing the integration of the TAMRA protons to the integration of the internal protons in the G5 PAMAM dendrimer (1210 protons).[7,29] The averages of n = 0.0, 0.9, 1.8, 3.3, 4.5, and 6.9 are in reasonable agreement with the UPLC data. The NMR values are less reliable than the UPLC values because (a) the isolated fraction does not fully represent the material used to determine the internal proton count of 1210, thus introducing error into the comparison of the integrated ratios, and (b) we are determining the ratio by comparing a small number of TAMRA protons to a large number of dendrimer protons. MALDI-TOF-MS was also used to characterize each isolated fraction (Supporting Information Table S1 and Figure S1). A trend toward higher mass was observed as n increased from 1 to 4 as well as for 5+; however, obtaining dye:dendrimer ratios from such data is inaccurate because we are sampling a different subfraction of the entire MW distribution for each G5-NH_2-TAMRA$_n$ (see the HPLC separation in Scheme 1b). The impact of the differential subfractionation is highlighted by the 300 Da decrease observed when comparing G5-NH_2-TAMRA$_o$ to G5-NH_2-TAMRA$_1$. In our previous work discussing the synthesis of related dye:dendrimer conjugates, we compared the relative ability of

DOI: 10.1021/bc5005735
Bioconjugate Chem. 2015, 26, 304−315

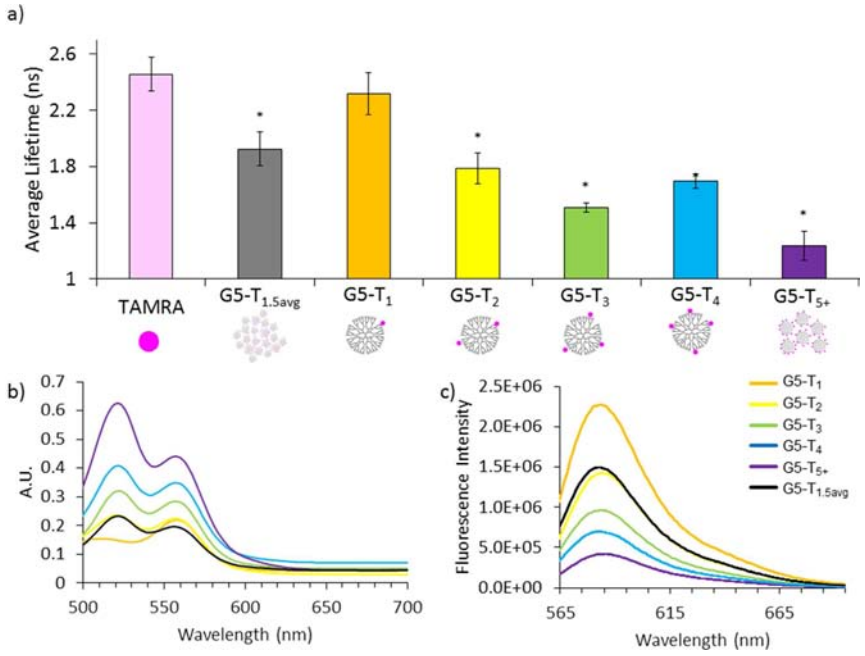

Figure 1. (a) Fluorescence lifetime values, (b) absorption spectra, and (c) emission spectra of 0.1 mg/mL G5-NH_2-TAMRA$_n$ (n = 0, 1, 2, 3, 4, 5+, 1.5$_{avg}$) in aqueous solution. A significant decrease in lifetime value (denoted by *) was observed for samples with $n > 1$ as compared to free TAMRA dye (pink) and G5-NH_2-TAMRA$_1$. The absorption increases while the emission decreases with increasing n. See Supporting Information Table S4 for p values. Error bars indicate std. dev. obtained from four measurements.

UPLC, ^{1}H NMR spectroscopy, and MALDI-TOF-MS data to assign dye:dendrimer ratios in detail.[14]

The impact of the dye:dendrimer ratio on photophysical properties was assessed using a combination of FLIM and absorption and emission spectroscopies (Figure 1). The absorption and emission spectra were obtained for 0.1 mg/mL G5-NH_2-TAMRA$_n$ solutions in water, which corresponds to roughly 3−4 μM solutions. As expected for this concentration of dye, the absorption spectrum for G5-NH_2-TAMRA$_1$ exhibited a single maximum at 560 nm.[14,30] Although the total solution concentration for dye in G5-NH_2-TAMRA$_2$ was still micromolar, the absorption now showed the classic two peak pattern, at 525 and 560 nm, typically associated with formation of TAMRA dimers in highly concentrated solutions.[30] This pattern provided additional evidence for the absence of $n \geq 2$ materials in the sample assigned as G5-NH_2-TAMRA$_1$. In addition, the relative intensity ratio of the 525 and 560 nm peaks indicated that little if any n = 1 material was present in the G5-NH_2-TAMRA$_2$ sample. The two peaks remained present, and the 525 nm peak grew in relative intensity as n increased. For all these samples, the local concentration of dye, which is restricted on each dendrimer particle to a hydrodynamic sphere of 3.1 nm radius,[31] was on the order of 10 M. The impact of the dye:dendrimer ratio was also observed in the fluorescence spectra taken in water. The most fluorescent material, as a function of dendrimer concentration, is G5-NH_2-TAMRA$_1$. It had roughly twice the fluorescence emission of G5-NH_2-TAMRA$_2$, which had twice as much dye, and three times the fluorescence emission of G5-NH_2-TAMRA$_4$, which had four times as much dye. G5-NH_2-TAMRA$_1$ also had roughly twice the fluorescence emission of stochastically prepared G5-NH_2-TAMRA$_{1.5(avg)}$, which consisted of n = 0, 1, 2, 3, 4, and 5 in percentages of 22%, 34%, 25%, 13%, 5%, and 1%, respectively. The impact of n is further demonstrated in the FLIM analysis. The fluorescence lifetime for free TAMRA in water (0.2 μM) was measured to be 2.5 ± 0.1 ns and a similar lifetime value for G5-NH_2-TAMRA$_1$ (0.2 μM) was obtained of 2.3 ± 0.2 ns. In all cases, increased dye:dendrimer ratios resulted in a decreased lifetime value as compared to G5-NH_2-TAMRA$_1$. The change was not linear, and G5-NH_2-TAMRA$_3$ had a lower lifetime value (1.5 ± 0.1 ns) than the G5-NH_2-TAMRA$_4$ (1.7 ± 0.1 ns) (Figure 1). Additional unexpected trends in lifetime values occurred when using the samples for cellular uptake and in biological environment modeling studies (vida infra). Fluorescence lifetime values for all samples in water, as well as for aqueous solutions with controlled ionic strength and biomolecule concentration, are provided in Supporting Information Table S2.

Cellular Uptake of Cationic Dendrimers: the Impact of Dye:Dendrimer Ratio. Fluorophore:polymer ratio has been reported to influence biological behavior;[22,24] however, the mechanism of these effects has been obscured by stochastic distributions of dye:dendrimer ratios. In this study, we focus on the real and apparent impacts of dye:dendrimer ratio on cellular uptake. As a model system, we employed mean fluorescence as measured by flow cytometry to quantify uptake in HEK293A cells. Cells were exposed to 0.5 μM G5-NH_2-TAMRA$_n$ (n = 1−4, 5+, 1.5$_{avg}$) for 3 h at 37 °C and mean fluorescence was determined by measurement of 10 000 cells (Figure 2). The raw mean fluorescence data exhibited the largest mean value for G5-NH_2-TAMRA$_1$ and the magnitude continued to decrease with increasing dye:dendrimer ratio; however, our independent measures of the fluorescence intensity of the conjugates (Figure 1) indicated that an accurate assessment of dendrimer uptake required a correction for the relative degree of fluorescence intensity for each conjugate.

In order to determine the correction factors, we measured the absorbance, emission, and lifetime characteristics of 0.1 mg/mL (3.5 μM) G5-NH_2-TAMRA$_n$ (n = 1, 2, 3, 4, 5+, 1.5$_{avg}$)

DOI: 10.1021/bc5005735
Bioconjugate Chem. 2015, 26, 304−315

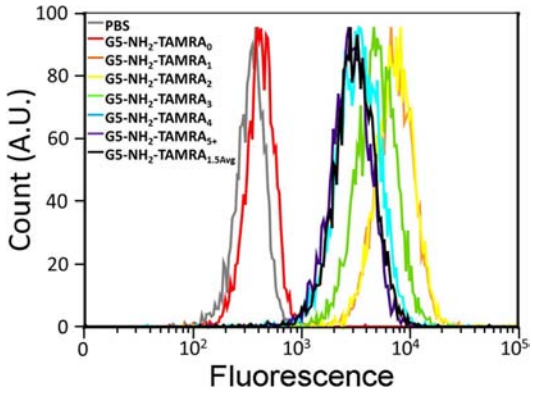

Figure 2. Flow cytometry of one repeat for the G5-NH_2-TAMRA$_n$ (n = 0, 1, 2, 3, 4, 5+, 1.5$_{avg}$) samples showing cell count versus fluorescence intensity.

solutions in a variety of aqueous solutions to model potential interactions from both salt and biomolecules. The measurements were performed in aqueous solution (Figure 1), NaCl, PBS, and undiluted fetal bovine serum (FBS). We also included controls containing bovine serum albumin (BSA) and glucose in water (at concentrations present in our FBS control) to independently evaluate the impact of these two components. Ficoll was used as a control for biomolecule crowding effects. The impact of interaction with negatively charged macromolecules was modeled using 1:1 and 1:10 N:P ratios of both plasmid DNA (pDNA) and antisense DNA (asDNA) (N is the number of dendrimer primary amines and P is the number of DNA phosphates). Finally, we employed HEK293A cell lysate at 100 000 cells per mL as a final, comprehensive control solution (Supporting Information Figures S2 and S3). The cell lysate was prepared by osmotically lysing cells followed by sonication. This lysate contains all of the cell lipids and protein and is detergent free, and thus differs from conventional lysates. For all conditions studied, G5-NH_2-TAMRA$_1$ exhibited the most intense fluorescence emission. In order to compare the emission intensities for the various conjugates under a given model condition, we defined the brightest emission of G5-NH_2-TAMRA$_1$ as 1 and determined the relative fraction of emission for the remaining conjugates (Table 2). The overall trend was a decrease in emission with increasing dye:dendrimer ratio. The overall magnitude of the nonquenched fluorescence varied greatly with the addition of the second dye (G5-NH_2-TAMRA$_2$), ranging from 93% for ficoll to 42% for PBS. When considering just the G5-NH_2-TAMRA$_n$ (n = 1, 2, 3, 4) fluorescence, the change in intensity as a function of n was monotonic; however, when the more complex n = 1.5$_{avg}$ and n = 5+ samples were considered, multiple deviations in the monotonic trend were associated with both samples. The origins of this complex fluorescence emission behavior are not clear. The data show the difficulty in extrapolating behavior for such heterogeneous mixtures of conjugated fluorophores. Fluorescence lifetime measurements for G5-NH_2-TAMRA$_1$ (2.3 ± 0.2 ns) and TAMRA (2.5 ± 0.1 ns) in water were essentially identical, and lifetimes decreased, as expected for the decrease in emission intensity, as a function of n. Based on these studies, we employed the fluorescence correction factors determined from aqueous solution, FBS solution (which also matched trends observed for the cell-based lifetime studies, vida infra), and cell lysate in order to correct the mean fluorescence values obtained from flow cytometry.

Application of the fluorescence emission correction factors (Table 2) to the mean fluorescence data obtained from flow cytometry (Figure 2) resulted in the trends in mean fluorescence illustrated in Figure 3. For each correction factor, the data for G5-NH_2-TAMRA$_1$ (G5-T$_1$) was normalized to the intensity observed for raw emission data. All three corrections trend in the same direction and indicate that the uptake of the $n \geq 2$ conjugates is significantly underestimated when only raw mean fluorescence data is considered. Indeed, the data indicate that *uptake does not decrease as a function of n* as implied by comparison of the raw mean fluorescence intensities. Rather, $n \geq 2$ conjugates give greater uptake than the n = 1 conjugate. These data also suggest that studies with dye conjugates overestimate the uptake rates of dye-free G5 PAMAM dendrimer into cells, although the rates may be a reasonable estimate for dendrimer containing other moieties of similar hydrophobicity, such as drugs. Finally, these data indicate that the use of raw mean fluorescence data to quantify dye uptake in vivo using stochastic dye:dendrimer, or more generally dye:polymer, conjugates can lead to errors of at least a factor of 3−5 if the biological fractionation effects on the materials are unknown.

Application of Dendrimer−TAMRA Conjugates for Fluorescence Lifetime Imaging Microscopy (FLIM). The G5-NH_2-TAMRA$_n$ (n = 1, 2, 3, 4, 5+, and 1.5$_{avg}$) conjugates varied in terms of fluorescence intensity as a function of n (Figures 1−3). The variation of intensity with n indicates that interpreting the uptake of materials into the cell using relative brightness in the confocal fluorescence images will not give reliable results (Figure 4). In this case, HEK293A cells were treated with 1 μM G5-NH_2-TAMRA$_n$ (n = 1, 2, 3, 4, 5+, and 1.5$_{avg}$) conjugates for 3 h. All treated cells exhibited a punctate distribution of fluorophore uptake (TAMRA = green), which

Table 2. Fluorescence Emission Intensity Characterization Summary for G5-NH_2-TAMRA$_n$ Material[a]

	fluorescence ratios for control solutions of 200 μM G5-NH_2-TAMRA$_n$							
	water	PBS	NaCl	BSA	ficoll	pDNA	FBS	asDNA
G5-(TAMRA)$_{1.5avg}$-NH_2	0.54	0.53	0.7	0.69	0.93	0.59	0.54	0.77
G5-(TAMRA)$_0$-NH_2	-	-	-	-	-	-	-	-
G5-(TAMRA)$_1$-NH_2	1	1	1	1	1	1	1	1
G5-(TAMRA)$_2$-NH_2	0.53	0.42	0.45	0.83	0.93	0.81	0.72	0.77
G5-(TAMRA)$_3$-NH_2	0.43	0.24	0.27	0.57	0.59	0.44	0.43	0.47
G5-(TAMRA)$_4$-NH_2	0.34	0.17	0.17	0.42	0.33	0.25	0.29	0.44
G5-(TAMRA)$_{5+}$-NH_2	0.22	0.18	0.21	0.42	0.51	0.2	0.26	0.31

[a]For each condition the intensity for G5-NH_2-TAMRA$_1$ is defined as 1 and the fractional intensity observed for each n = 2, 3, 4, 5+, and 1.5$_{avg}$ is indicated.

DOI: 10.1021/bc5005735
Bioconjugate Chem. 2015, 26, 304−315

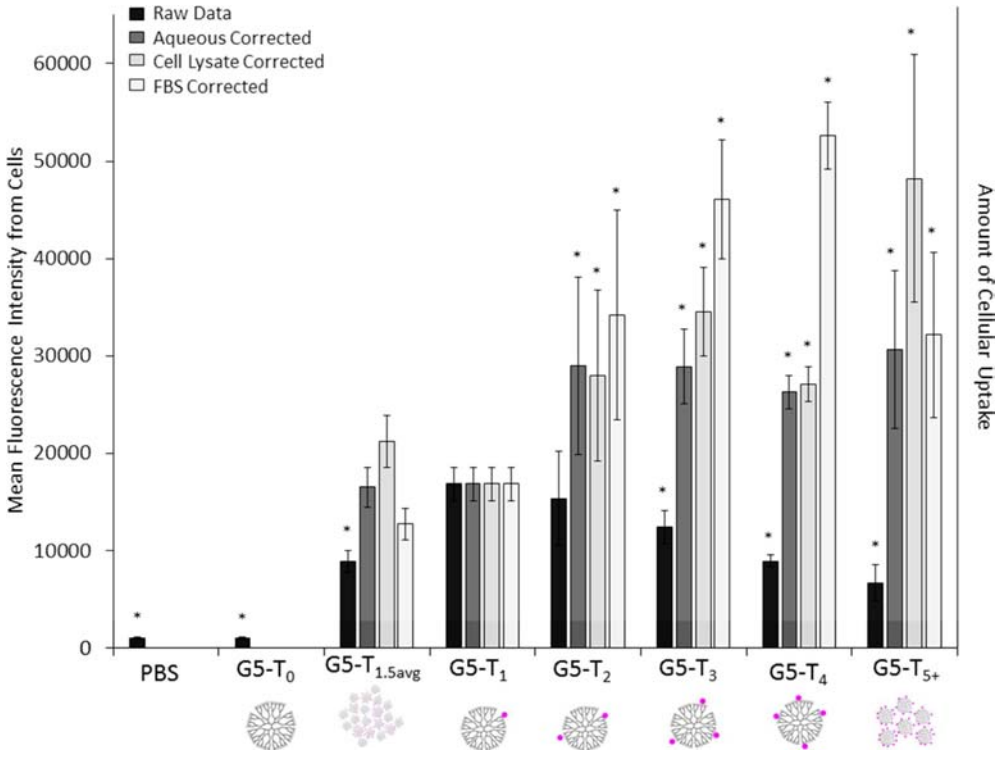

Figure 3. Uptake and binding of G5-NH_2-TAMRA$_n$ as measured by flow cytometry after 3 h of incubation with HEK293A cells. The bar graphs illustrate the uptake trend as measured by raw mean fluorescence data and the trends after correction using relative fluorescence emission in aqueous solution, FBS solution, and cell lysate. All correction factors are summarized in Table 2 from the data shown in Figure 1c and Supporting Information Figures S2 and S3). Significance for differences in G5-NH_2-TAMRA$_n$ fluorescence intensity (denoted by *) as compared to G5-NH_2-TAMRA$_1$ intensity was assessed using a Games-Howell analysis (see Supporting Information Table S4 for p values). Error bars indicate std. dev. obtained from twelve measurements (triplicate runs of four biologically independent experiments).

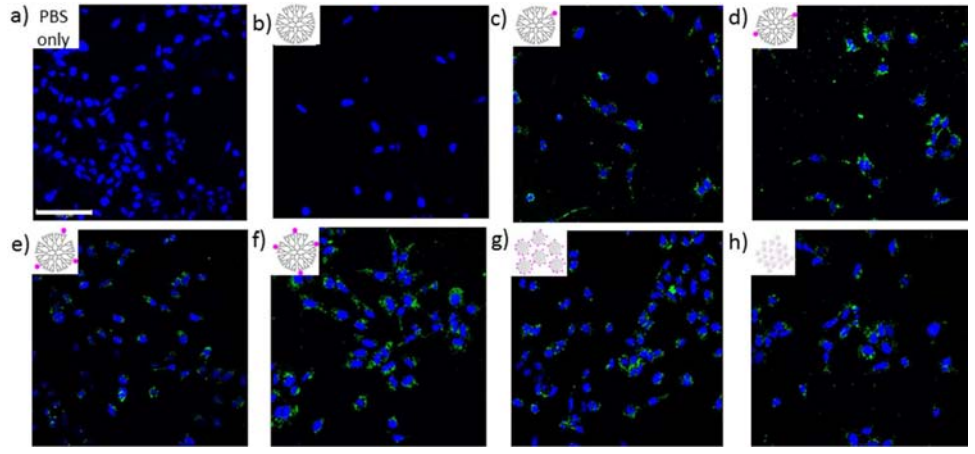

Figure 4. Confocal microscopy images of HEK293A cells incubated for 3 h with (a) PBS only, (b) G5-NH_2, (c) G5-NH_2-TAMRA$_1$, (d) G5-NH_2-TAMRA$_2$, (e) G5-NH_2-TAMRA$_3$, (f) G5-NH_2-TAMRA$_4$, (g) G5-NH_2-TAMRA$_{5+}$, and (h) G5-NH_2-TAMRA$_{1.5avg}$. TAMRA fluorescence is shown in green. The fluorescence deriving from DAPA-stained cell nuclei is shown in blue. Images were obtained with a 40× oil immersion objective. The same set of image locations is presented in Figure 5 using FLIM. Scale bar is 100 μm.

was in general agreement with the flow cytometry data (Figures 2 and 3). The mixtures G5-NH_2-TAMRA$_{5+}$ (Figure 4g) and G5-NH_2-TAMRA$_{1.5avg}$ (Figure 4h) were expected to contain fluorescent particles with intensity levels varying by up to a factor of 5. Therefore, even within a given cell or field of cells, relative intensity variation may not be correlated with extent of uptake.

FLIM offers an alternative method of fluorescence image contrast that is generally insensitive to intensity-based artifacts. In addition, the fluorescence lifetimes measured are sensitive to the microenvironment including pH, ion concentration, and molecular association.[32] FLIM images were obtained for the same locations as the confocal microscopy data presented in Figure 4. The G5-NH_2-TAMRA$_{1.5avg}$ treated sample (Figure 5h) gave an average lifetime of 0.7 ± 0.2 ns which is significantly lower than the 1.9 ± 0.1 ns obtained for aqueous solution. This value is also substantially lower than observed for all other samples with the exception of G5-NH_2-TAMRA$_4$. The

DOI: 10.1021/bc5005735
Bioconjugate Chem. 2015, 26, 304−315

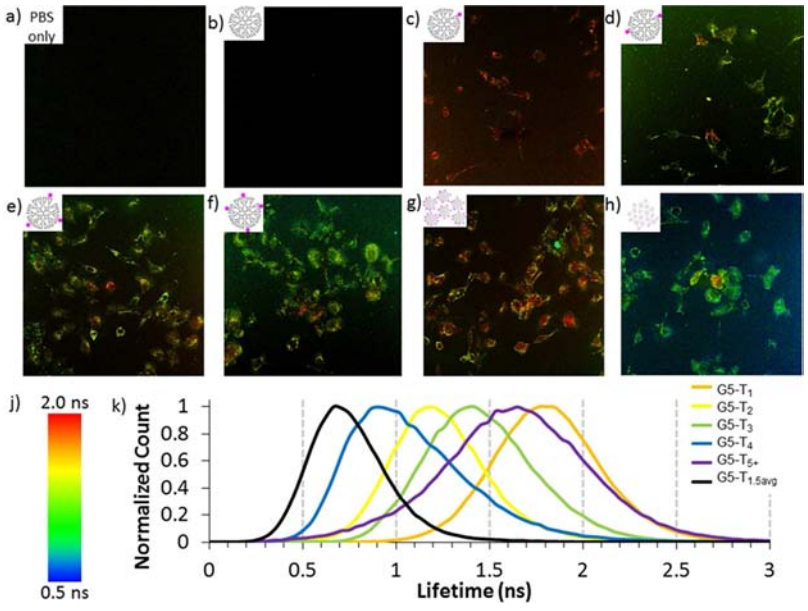

Figure 5. FLIM images of HEK293A cells incubated for 3 h with (a) PBS only, (b) G5-NH_2, (c) G5-NH_2-TAMRA$_1$, (d) G5-NH_2-TAMRA$_2$, (e) G5-NH_2-TAMRA$_3$, (f) G5-NH_2-TAMRA$_4$, (g) G5-NH_2-TAMRA$_{5+}$, and (h) G5-NH_2-TAMRA$_{1.5avg}$. (j) Color code for FLIM images. (k) Histograms of fluorescence lifetimes for FLIM images. Images were obtained with a 40× oil immersion objective. The same set of image locations is presented in Figure 4 using confocal fluorescence microscopy.

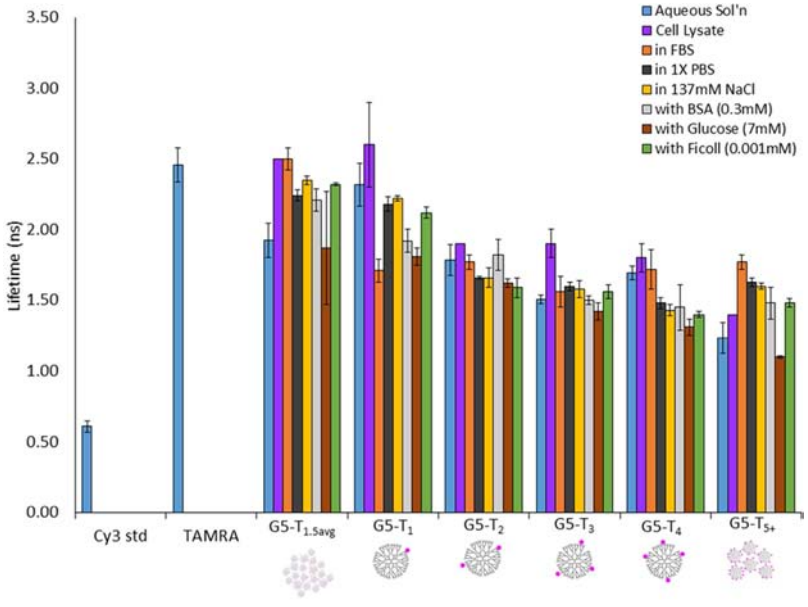

Figure 6. Fluorescence lifetime measurements of G5-NH_2-TAMRA$_n$ (n = 0, 1, 2, 3, 4, 5+, 1.5$_{avg}$) in aqueous solution under various conditions. Cy3 and TAMRA dyes in water were used as calibration standards. See Supporting Information Table S2 for summary of numerical values. Error bars indicate std. dev. obtained from four measurements.

G5-NH_2-TAMRA$_1$ treated cells exhibited uniformly higher lifetimes of 1.8 ± 0.5 ns (Figure 5c), which itself was substantially lower than the 2.3 ± 0.2 ns observed in aqueous solution. Despite the fact that the G5-NH_2-TAMRA$_{1.5avg}$ sample contained 34% G5-NH_2-TAMRA$_1$, the 1.8 ns lifetimes associated with T_1 material did not appear in the cell images (Figure 5h). The G5-NH_2-TAMRA$_{5+}$ treated cells also exhibited among the highest lifetime value with an average of 1.6 ± 0.6 ns. Surprisingly, this value was greater than the average values observed for G5-NH_2-TAMRA$_n$ (n = 2, 3, 4), as well as for the G5-NH_2-TAMRA$_{5+}$ aqueous value of 1.2 ± 0.1 ns. The images from Figure 5 are provided in large form in Supporting Information Figure S4. Images of individual cells measured using a 40× oil objective with an additional optical zoom of 6.25× are provided in Supporting Information Figure S5 and the graphical abstract to further illustrate the various intracellular lifetimes observed with these materials. The lifetimes in the zoomed images show a similar trend to the nonzoomed images. The zoomed-in images highlight the punctate distribution of the G5-TAMRA within cells. Further experiments with markers for cellular organelles are needed to determine if samples with different dye:dendrimer ratios are transported to different organelles. The observation that most of the samples exhibited dynamic quenching in the cell,

DOI: 10.1021/bc5005735
Bioconjugate Chem. 2015, 26, 304−315

resulting from possible environmental differences such as pH, ionic strength, or biomolecule interactions, was expected. It was surprising that the G5-NH_2-TAMRA$_{1.5avg}$ treated cells did not show the full range of lifetimes represented by the dye:dendrimer ratios present and that the lifetime of G5-NH_2-TAMRA$_{5+}$ increased in cells, indicating a reduction in dynamic quenching.

In order to gain a greater understanding of how these changes in lifetime varied as a function of *n*, a series of control experiments were carried out. Fluorescence lifetimes were measured for solutions of G5-NH_2-TAMRA$_n$ (n = 1, 2, 3, 4, 5+, and 1.5$_{avg}$) in cell lysate, 1× PBS, 137 mM NaCl, 0.3 mM BSA, 7.0 mM glucose, 0.001 mM ficoll, and undiluted fetal bovine serum (FBS) (Figure 6). Additional lifetime measurements were made for aqueous solutions using pH 3 and 5 buffers and for aggregates of G5-NH_2-TAMRA$_n$ (n = 1, 2, 3, 4, 5+, and 1.5$_{avg}$) generated by mixing with anionic oligonucleotides (both plasmid and antisense DNA) (Supporting Information Figures S6 and S7). The undiluted FBS was used to generate a high concentration of biomolecules comparable to that found in the cellular environment. The concentrations of NaCl, BSA, and glucose were set to the levels of the FBS control. Ficoll was set at 5 equiv per dendrimer. 1× PBS is a standard buffer system with an overall salt concentration similar to that of blood and the same NaCl concentration as the FBS.

The FBS control best matched the cell FLIM data, as it gave both the increase in dynamic quenching (lower lifetime) of the G5-NH_2-TAMRA$_1$ material and the decrease in dynamic quenching (higher lifetime) observed for G5-NH_2-TAMRA$_{5+}$ (Figure 6). In order to understand how the components of FBS might lead to these lifetime changes, solutions were tested containing salt (PBS, NaCl) and biomolecule components (BSA, glucose) as well as a ficoll. The results point to a complex mixture of static and dynamic quenching mechanisms present in the G5-NH_2-TAMRA$_n$ conjugates. For G5-NH_2-TAMRA$_1$, NaCl and PBS alone or the presence of ficoll did not generate a significant change in fluorescence lifetime; however, both BSA and glucose did cause a change. For G5-NH_2-TAMRA$_{5+}$, NaCl, PBS, BSA, and ficoll all caused a significant increase in fluorescence lifetime, although glucose did not. For both G5-NH_2-TAMRA$_n$ (n = 2, 3), little change in fluorescence lifetime was observed for any simple controls, although cell lysate caused a significant increase in lifetime for n =3. For G5-NH_2-TAMRA$_4$, all conditions but FBS and cell lysate were observed to decrease lifetime. Since fluorescence lifetime is also known to change for a fluorophore based on pH,[33] the conjugates were also measured in pH = 3, 5, and 7 aqueous buffers. Treatment of G5-NH_2-TAMRA$_1$ with pH 3 and 5 buffers caused no change in lifetime, whereas both buffers resulted in an increase in lifetime for G5-NH_2-TAMRA$_{5+}$ (Supporting Information Figure S6 and Table S3). No clear lifetime trends were observed for the impact of aggregate formation induced by plasmid and antisense DNA, although a decrease in lifetime for G5-NH_2-TAMRA$_1$ and an increase in lifetime for G5-NH_2-TAMRA$_{5+}$ were again observed (Supporting Information Figure S7 and Table S3). These observations can be compared to the measurements of TAMRA fluorescence lifetime of 2.28 ± 0.01 ns in buffer and 2.48 ± 0.01 ns on a DNA aptamer.[34]

The cell FLIM data can be rationalized in part based upon the control experiments. The most surprising result, the increase of fluorescence lifetime for G5-NH_2-TAMRA$_{5+}$ in HEK293A cells, was reproduced under a variety of control conditions. This behavior may result from a dye−dye static quenching interaction present in a fraction of the G5-NH_2-TAMRA$_{5+}$ sample. Upon addition of salt and biomolecules, the dye−dye interactions may be broken up leading to a lifting of the static quenching and the observation of a new, longer lifetime value. In addition, the salt and biomolecule interaction with the dye may change the nature of the dynamic quenching that leads to the 1.2 ± 0.1 ns lifetime in aqueous solution, which could also lead to an increase in observed lifetime. This balancing of effects only appears operative for $n \geq 5$ dyes per G5 PAMAM dendrimer.

Many previous studies have demonstrated that the punctate G5 PAMAM dendrimer distribution in cells arises from localization into endosomes and lysomes;[35] however, the control data for pH effects (Supporting Information Figure S6) does not explain the decrease in lifetimes observed in the FLIM images (Figure 5 and Supporting Information Figure S4). Based on our series of control experiments, it appears that changes in ionic strength or interactions with other biomolecules present in the endosomes or lysomes are more likely causes of the decreased fluorescence lifetimes for these dye:dendrimer conjugates in the HEK293A cells.

■ CONCLUSIONS

G5-NH_2-TAMRA$_n$ (n = 1−4, 5+, 1.5$_{avg}$) samples have been synthesized and characterized by UPLC, ^{1}H NMR, and MALDI-TOF-MS. The absorbance, fluorescence emission, and fluorescence lifetime properties have been measured in aqueous solution as well as in a variety of biologically relevant control conditions. By preparing this set of dye:dendrimer conjugates with well-defined dye:dendrimer ratios, we hope to elucidate the behaviors of the stochastic mixtures of dye:dendrimer ratios typically employed to understand cationic polymer uptake and localization.

During the course of this study we showed that dendrimer uptake varied as a function of *n*. In addition, knowledge of how fluorescence intensity for G5-NH_2-TAMRA$_n$ varies as a function of n is required for properly understanding the relative degree of uptake. These observations raise the greatest concerns for studies in which a stochastic mixture can be "separated" by the interaction with the biological systems, i.e., exhibit a hydrophobic dependency on biodistribution,[15,19,25,26] and when biological tissues are evaluated for uptake by fluorescence without knowledge of the fraction of the dye:polymer conjugate present. Thus, for materials containing stochastic dye:polymer distributions, hypothesis H1 that the uptake of cationic polymer can be quantified by the change in mean fluorescence of cells should be used with caution. For low Stokes shift dyes similar to TAMRA and fluorescein, H1 is not valid.

The FLIM studies of G5-NH_2-TAMRA$_n$ resulted in a surprising set of lifetime images. In particular, the observation of both decreasing and increasing lifetimes for a given environmental condition as a function of n was not expected. In addition, the magnitudes of changes seen as a function of n for a given control environment was similar to the magnitude of change observed for constant n as a function of changing the environment. This indicates that interpretations of fluorescence lifetimes as resulting from changes in biological environment must be approached with great caution for stochastic dye:polymer conjugates, particularly if biological fractionation of the samples has taken place. In contrast to the initial hypothesis (H2), the components of a stochastic distribution of dye:polymer ratios do not have a similar collective trend in

DOI: 10.1021/bc5005735
Bioconjugate Chem. 2015, 26, 304−315

terms of environmental lifetime response. Furthermore, with respect to H3, variation in dye:polymer ratio is found to have a similar magnitude of impact on fluorescence lifetime as changes in the biological environment.

Upon testing the three hypotheses, it is clear that caution needs to be taken when using dye:polymer mixtures to determine cellular uptake and fluorescence lifetime. One good solution for achieving linear intensity profiles is the use of large Stokes shift dyes, as discussed by Mier et al.[16] The strategy of using a stochastic mixture that contains very little of zero dye and one dye on the polymer, as delineated by Schroeder et al., can also provide a solution.[17] However, many scientifically and technologically important dyes (i.e., TAMRA, fluorescein, AlexaFluors, etc.) have small Stokes shifts, and dye substitution is not always a favorable option. Since dye:polymer ratio impacts biodistribution and function,[9−12,15−17,19−27] creation of a high mean stochastic ratio is not a general solution to the problem. In these cases, either direct synthesis of precise dye:polymer materials[36−38] or physical separation to obtain precise dye:polymer ratios[7,8,14,29] is needed for quantitative uptake or lifetime studies.

EXPERIMENTAL PROCEDURES

Chemicals and Methods. Biomedical grade G5 PAMAM dendrimer was purchased from Dendritech Inc. and purified using rp-HPLC to give a molecular weight fraction free of trailing generations (G1-G4) as well as G5 dimers and higher oligomers.[28] Trifluoroacetic acid, HPLC grade water, GE PD-10 Sephadex columns, and HPLC grade acetonitrile were purchased from Fisher-Scientific and used as received. 5-Carboxy tetramethylrhodamine succinimydyl ester (TAMRA) was purchased from Life Technologies. A 500 MHz Varian NMR instrument was used for all ^{1}H and ^{19}F NMR measurements. All MALDI-TOF MS measurements were performed on a Bruker Ultraflex III with sinapinic acid matrix (Sigma-Aldrich) and sodium trifluoroacetate (Fischer Scientific) salt sample preparation. Serum-free DMEM (SFM) from life technologies was employed for cell culture of HEK293A cells, which were obtained from ATCC. Complete medium was made by adding 50 mL of fetal bovine serum (FBS) and 5 mL 100× of penicillin−streptomycin to 500 mL of SFM.

Conjugation of TAMRA to G5 PAMAM Dendrimer. TAMRA (0.0121 g, 0.023 mmol, 4.5 equiv) was dissolved in dimethyl sulfoxide (3.0 mL) and added dropwise to a stirred solution of G5 PAMAM dendrimer (0.1390 g, 0.0050 mmol, 1.0 equiv) dissolved in water (30.0 mL). The mixture was stirred at 20 °C overnight and purified using a GE PD-10 sephadex column. A pink solid was obtained after removal of solvent (75% yield). The product was characterized using ^{1}H NMR, UV−vis absorption and fluorescence spectroscopy, analytical rp-UPLC, and MALDI-TOF MS.

Isolation of Material Containing Precise TAMRA/Dendrimer Ratios. Semipreparative rp-HPLC isolation was carried out on a Waters Delta 600 HPLC. For analysis of the dendrimer and conjugates, a C18 silica-based rp-HPLC column (250 × 21.20 mm, 10 μm particles) connected to a C18 guard column (50 × 21.20 mm) was used. The mobile phase for elution of the conjugates was a linear gradient beginning with 95:5 (v/v) water/acetonitrile and ending with 65:35 (v/v) water/acetonitrile over 28 min at a flow rate of 12.00 mL/min. Trifluoroacetic acid (TFA) at 0.10 wt % concentration in both water and acetonitrile was used as a counterion to make the dendrimer surfaces hydrophobic. Elution traces of the dendrimer−ligand conjugate were obtained at 210 nm. A concentration of 24 mg/mL per injection was used. 120 fractions of 6 s duration were collected starting at 9 min and 30 s. Selection of fractions for combination to yield the precise TAMRA:dendrimer ratios was based upon analysis of the chromatogram in Origin-Pro. Each isolated combination of fractions was reinjected onto an analytical UPLC to determine purity of the sample. ^{1}H NMR spectra are provided in Supporting Information Figure S8.

Analytical Reverse Phase Ultra Performance Liquid Chromatography (rp-UPLC). Purity of G5-NH_2-TAMRA$_n$ materials was assessed at 210 nm (dendrimer absorption wavelength) using a Waters Acquity UPLC system controlled by Empower 2 software. A C18 silica-based column (Phenomenex) was employed with a mobile phase linear gradient beginning with 95:5 (v/v) water/acetonitrile and ending with 55:45 (v/v) water/acetonitrile over 17 min at a flow rate of 3.0 mL/min. Trifluoroacetic acid (TFA) at 0.14 wt % concentration in water and acetonitrile was used as a counterion to make the dendrimer surfaces hydrophobic.

Absorption and Emission Measurements. Fluorescence (Fluoromax-4) and UV−vis (Shimadzu UV-1601) measurements were taken at a concentration of 0.1 mg/mL. For all measurements, the concentration of the solutions was 0.1 mg/mL and within an error of ±0.02. For the fluorescence measurements an excitation of 530 nm and emission of 580 nm were used with a slit width of 2 nm.

MALDI-TOF-MS Measurements. Three solutions were prepared: (1) 10 mg/mL dendrimer in water, (2) 20 mg/mL sinapinic acid in 1:1 (v/v) acetonitrile:water, and (3) 20 mg/mL sodium trifluoroacetate in water. These were then combined in a ratio of 10:2:1 of matrix:dendrimer:salt solution. The plate was spotted with 1 μL volumes of solution and allowed to dry. At least 100 scans were averaged per measurement and a smoothing factor of 12 channels was employed.

Cell Culture Materials. DMEM high glucose with sodium pyruvate and glutamine (Life Technologies Inc.) was the base media. Complete media was made by adding 50 mL of FBS, 5 mL of Nonessential Amino Acids (Thermo Scientific), and 5 mL of penicillin−streptomycin to 500 mL DMEM. PBS (1×) without Ca^{2+} and Mg^{2+} was obtained from Life Technologies. Cells were maintained at 37 °C with 5% CO_2 in a humidified atmosphere and subcultured by trypsinization (Life Technologies).

Measurement of G5-NH_2-TAMRA$_n$ Binding and Uptake in HEK293A Cells Using Flow Cytometry. HEK 293 A cells were seeded in 12 well plates (Fisher Scientific, 3.8 cm^2) at a density of 150 000 cells per well in 1 mL of complete DMEM and incubated overnight at 37 °C with 5% CO_2. The complete media was removed prior to incubation with G5-NH_2-TAMRA$_n$. The cells were then rinsed with 1 mL of PBS, followed by addition of 0.8 mL of SFM. The cells were incubated for 3 h at 37 °C with 0.5 μM G5-NH_2-TAMRA$_n$ (n = 0−4, 5+, 1.5_{avg}) (~5.0 μL volume of 2 mg/mL solution added to each well). Each treatment was run in triplicate, and 4 independent biological repeats were performed. After incubation with G5-NH_2-TAMRA$_n$ material, the HEK293A cells were rinsed with PBS and harvested for flow cytometry by trypsinization. Trypsinization was performed by incubation with 200 μL of trypsin for 2 min at 37 °C. After 2 min, 0.8 mL cold PBS was added to each well to inhibit the trypsin, and the suspensions were then centrifuged for 5 min at 2000 rpm. Cell

DOI: 10.1021/bc5005735
Bioconjugate Chem. 2015, 26, 304−315

pellets were resuspended in 400 μL of PBS. Cell fluorescence was measured using a BD C6 Accuri flow cytometer by collecting 10 000 events per sample. The cells were excited using a 488 nm laser and emission at the 585 ± 20 nm region was measured. Differences were determined according to a post hoc Games-Howell test using predictive analytics SPSS software. This statistical test was chosen because it does not assume equal variance, which we deemed most relevant for comparing multiple biological replicates of HEK 293A cells (* used in figures indicates a p value <0.05).

Cell Preparation for Confocal and Fluorescence Lifetime Microscopy. HEK 293 A cells were seeded in 2 well confocal chambers (Nunc Labtek II, 4 cm^2) at a density of 50 000 cells per well in 1.5 mL of complete DMEM and incubated overnight at 37 °C with 5% CO_2. The complete media was removed prior to incubation with G5-NH_2-TAMRA$_n$. The cells were then rinsed with 1 mL of PBS, followed by addition of 0.5 mL serum free DMEM. Cells were incubated with 1 μM G5 TAMRA in serum free DMEM for 3 h. The cells were then rinsed with PBS three times and fixed using 2% paraformaldehyde. The fixed cells were rinsed 3 times with PBS, two drops of prolong gold solution containing DAPI was added, and a 1.5 thickness coverslip was placed on each sample.

Confocal Fluorescence Microscopy. Confocal microscopy was performed using Leica SP5 inverted confocal microscope using a 40× oil immersion objective. The section thickness was set at 1 μm. The excitation wavelength used was 555 nm, and the emission from 585 to 700 nm was measured.

Time Domain Fluorescence Lifetime Imaging Microscopy (FLIM) of G5-NH_2-TAMRA$_n$ in HEK 293A Cells Using a Multiphoton Laser. Lifetime imaging for HEK293A cells was performed using a LEICA inverted SP5 confocal microscope in the multiphoton mode. The source was a Mai-Tai laser with a 20 MHz frequency. The excitation wavelength was 850 nm with 2.2 W power. A PMT detector and TCSPC counter were used to measure lifetime. Images shown were taken at approximately midcell height by first taking an image in the $x-z$ plane and using the DAPI signal to estimate cell heights (about 8 μm for the HEK293A cells). The z position was then set to this value, and the $x-y$ plane images shown in Figure 5 were obtained. Taking images too near the confocal chamber or coverslip surface induced low lifetime artifacts. Measurements were taken until a maximum of 1000 photons were measured for each pixel. The lifetime histograms and exponential fitting were performed using Symphotime software (Picoquant Inc.). The FLIM images of cells presented here show the average lifetime per pixel calculated using the FastFLIM algorithm in Symphotime. For solution lifetimes, single exponential lifetimes were used. It has been reported that the lifetime of TAMRA changes with temperature.[39] In our experiments, the MP laser could heat samples and change lifetimes. To test for this, the lifetimes for free TAMRA and G5-NH_2-TAMRA$_1$ were measured using two sequential 4 min scans (the average time to image a field of cells) to test if heating during image acquisition was affecting measured lifetime values. For free TAMRA, the sequentially measured lifetime values were 2.37 and 2.36 ns. For G5-NH_2-TAMRA$_1$, the values were 2.46 and 2.40 ns. These results indicate that change in lifetime due to temperature is not a cause for concern in our study.

Fluorescence Lifetime Imaging Microscopy (FLIM) Measurement of G5-NH_2-TAMRA$_n$ Lifetime Using Single Photon Laser Excitation. Lifetime imaging in solution was performed using an Olympus IX-81 time-resolved confocal microscope using avalanche photodiodes. The source was a SC-400-6-PP supercontinuum laser with 20 MHz frequency. The excitation wavelength was 530 nm with 6.0 W power. An APD detector and TCSPC counter were used to measure lifetime. The lifetime histograms and exponential fitting were performed using ALBA software. Single exponential fitting was performed to obtain solution lifetimes. The mean fluorescence intensity and fluorescence lifetime of each sample was measured. One-way ANOVA followed by Games-Howell post hoc analysis was performed to test if the means were significantly different.

Solution Conditions to Measure Control Fluorescence Lifetimes FLIM. Control measurements in water, 1× PBS, undiluted FBS (Thermo Fisher Scientific), NaCl (137 mM), BSA (23 mg/mL), glucose (1.25 mg/mL), and ficoll (60 mg/mL) were performed using 200 μM G5-NH_2-TAMRA$_n$. Polyplex solutions were mixed at an N:P of 10:1 and 1:1 at a concentration of 500 nM G5-NH_2-TAMRA$_n$ based on published protocols.[40]

Preparation of Cell Lysate. HEK 293A cell lysate was prepared by washing a confluent plate of cells with 1× PBS. The cells were then treated with 2 mL trypsin for 2 min at 37 °C. The trypsinization was stopped by adding 8 mL of complete DMEM. The cells were triturated and counted using a hemocytometer. The cells were centrifuged at 1400 g for 2 min and the supernatant was removed. The cells were then suspended in DI water such that there were 5 million cells per mL and sonicated in a bath sonicator for 15 min. The absence of intact cells was checked using a light microscope. For use in experiments, the lysate was diluted to 100 000 cells/mL. This protocol was used rather than typical cell lysate protocols in order to avoid detergents, which interfere with fluorescence lifetime solution measurements, and to include all cell lipid.

■ ASSOCIATED CONTENT

Supporting Information

Characterization data, fluorescence lifetime, p-values, MALDI-TOF-MS spectra, fluorescence emission spectra, FLIM images, NMR spectra. This material is available free of charge via the Internet at http://pubs.acs.org.

■ AUTHOR INFORMATION

Corresponding Author

*E-mail: mbanasza@umich.edu.

Author Contributions

Casey A. Dougherty and Sriram Vaidyanathan contributed equally to this work. C.A.D. performed synthesis, chromatography, mass spectrometry, NMR experiments, and flow cytometry, and contributed to lifetime imaging in solution. S.V. conducted the lifetime imaging in cells, contributed to lifetime imaging in solution, and also to flow cytometry experiments. C.A.D., S.V., B.G.O., and M.M.B.H. designed the experiments, analyzed data, and contributed to the writing of the manuscript.

Notes

The authors declare no competing financial interest.

■ ACKNOWLEDGMENTS

C.A.D., S.V., B.G.O., and M.M.B.H. acknowledge the University of Michigan Medical Center's Microscopy and Imaging Analysis Center (MIL) and the University of Michigan Single

DOI: 10.1021/bc5005735
Bioconjugate Chem. 2015, 26, 304−315

Molecule Analysis in Real Time (SMART) Center for use of their instruments to obtain confocal and lifetime imaging data, and the Michigan Nanotechnology Institute for Medicine and Biological Sciences (MNIMBS) for use of their flow cytometer to obtain cellular uptake data. J. Swanson is thanked for helpful discussions. This project has been funded in part with federal funds from the National Institutes of Health, National Institute of Biomedical Imaging and Bioengineering, under Award EB005028 and the Michigan Initiative for Innovation and Entrepreneurship (MIIE) Fund.

■ ABBREVIATIONS

G5 PAMAM, Generation 5 poly(amidoamine); TAMRA, 5-succidimidyl ester carboxy-tetramethylrhodamine; FLIM, fluorescence lifetime imaging microscopy

■ REFERENCES

(1) Larson, N., and Ghandehari, H. (2012) Polymeric conjugates for drug delivery. *Chem. Mater. 24*, 840−853.
(2) Lee, C. C., MacKay, J. A., Frechet, J. M. J., and Szoka, F. C. (2005) Designing dendrimers for biological applications. *Nat. Biotechnol. 23*, 1517−1526.
(3) Haag, R., and Kratz, F. (2006) Polymer therapeutics: concepts and applications. *Angew. Chem., Int. Ed. 2006*, 1198−1215.
(4) Mintzer, M. A., and Grinstaff, M. W. (2011) Biomedical applications of dendrimers: a tutorial. *Chem. Soc. Rev. 40*, 173−190.
(5) Mintzer, M. A., and Simanek, E. E. (2009) Nonviral vectors for gene delivery. *Chem. Rev. 109*, 259−302.
(6) Chen, M. J., and Yin, M. Z. (2014) Design and development of fluorescent nanostructures for bioimaging. *Prog. Polym. Sci. 39*, 365−395.
(7) Mullen, D. G., Fang, M., Desai, A., Baker, J. R., Orr, B. G., and Holl, M. M. B. (2010) A quantitative assessment of nanoparticle-ligand distributions: implications for targeted drug and imaging delivery in dendrimer conjugates. *ACS Nano 4*, 657−670.
(8) Mullen, D. G., and Banaszak Holl, M. M. (2011) Heterogeneous ligand-nanoparticle distributions: a major obstacle to scientific understanding and commercial translation. *Acc. Chem. Res. 44*, 1135−1145.
(9) Alexis, F., Pridgen, E., Molnar, L. K., and Farokhzad, O. C. (2008) Factors affecting the clearance and biodistribution of polymeric nanoparticles. *Mol. Pharmaceutics 5*, 505−515.
(10) Duan, X. P., and Li, Y. P. (2013) Physicochemical characteristics of nanoparticles affect circulation, biodistribution, cellular internalization, and trafficking. *Small 9*, 1521−1532.
(11) Moyano, D. F., Goldsmith, M., Solfiell, D. J., Landesman-Milo, D., Miranda, O. R., Peer, D., and Rotello, V. M. (2012) Nanoparticle hydrophobicity dictates immune response. *J. Am. Chem. Soc. 134*, 3965−3967.
(12) van Dongen, M., Dougherty, C. A., and Banaszak Holl, M. M. (2014) Multivalent polymers for drug delivery and imaging: the challenges of conjugation. *Biomacromolecules 15*, 3215−3234.
(13) Duhamel, J. (2014) Global analysis of fluoresence decays to probe the internal dynamics of fluorescently labeled macromolecules. *Langmuir 30*, 2307−2324.
(14) Dougherty, C. A., Furgal, J. C., van Dongen, M. A., Goodson, T., Holl, M. M. B., Manono, J., and DiMaggio, S. (2014) Isolation and characterization of precise dye/dendrimer ratios. *Chem.—Eur. J. 20*, 4638−4645.
(15) Pansare, V. J., Hejazi, S., Faenza, W. J., and Prud'homme, R. K. (2012) Review of long-wavelength optical and NIR imaging materials: contrast agents, fluorophores, and multifunctional nano carriers. *Chem. Mater. 24*, 812−827.
(16) Wangler, C., Moldenhauer, G., Saffrich, R., Knapp, E. M., Beijer, B., Schnolzer, M., Wangler, B., Eisenhut, M., Haberkorn, U., and Mier, W. (2008) PAMAM structure-based multifunctional fluorescent conjugates for improved fluorescent labelling of biomacromolecules. *Chem.—Eur. J. 14*, 8116−8130.
(17) Kim, Y., Kim, S. H., Tanyeri, M., Katzenellenbogen, J. A., and Schroeder, C. M. (2013) Dendrimer probes for enhanced photostability and localization in fluorescence imaging. *Biophys. J. 104*, 1566−1575.
(18) Opitz, A. W., Czymmek, K. J., Wickstrom, E., and Wagner, N. J. (2013) Uptake, effux, and mass transfer coefficient of fluorescent PAMAM dendrimers into pancreatic cancer cells. *Biochem. Biophys. Acta 1828*, 294−301.
(19) He, C. B., Hu, Y. P., Yin, L. C., Tang, C., and Yin, C. H. (2010) Effects of particle size and surface charge on cellular uptake and biodistribution of polymeric nanoparticles. *Biomaterials 31*, 3657−3666.
(20) Santos, J. L., Oliveira, H., Pandita, D., Rodrigues, J., Pego, A. P., Granja, P. L., and Tomas, H. (2010) Functionalization of poly(amidoamine) dendrimers with hydrophobic chains for improved gene delivery in mesenchymal stem cells. *J. Controlled Release 144*, 55−64.
(21) Shakhbazau, A., Isayenka, I., Kartel, N., Goncharova, N., Seviaryn, I., Kosmacheva, S., Potapnev, M., Shcharbin, D., and Bryszewska, M. (2010) Transfection efficiencies of PAMAM dendrimers correlate inversely with their hydrophobicity. *Int. J. Pharm. 383*, 228−235.
(22) Vuorimaa, E., Urtti, A., Seppanen, R., Lemmetyinen, H., and Yliperttula, M. (2008) Time-resolved fluorescence spectroscopy reveals functional differences of cationic polymer-DNA complexes. *J. Am. Chem. Soc. 130*, 11695−11700.
(23) Ketola, T. M., Hanzlikova, M., Urtti, A., Lemmetyinen, H., Yliperttula, M., and Vuorimaa, E. (2011) Role of polyplex intermediate species on gene transfer efficiency: polyethylenimine-DNA complexes and time-resolved fluorescence spectroscopy. *J. Phys. Chem. B 115*, 1895−1902.
(24) Yoo, H., and Juliano, R. L. (2000) Enhanced delivery of antisense oligonucleotides with fluorophore-conjugated PAMAM dendrimers. *Nucleic Acids Res. 28*, 4225−4231.
(25) Seib, F. P., Jones, A. T., and Duncan, R. (2006) Establishment of subcellular fractionation techniques to monitor the intracellular fate of polymer therapeutics I. Differential centrifugation fractionation B16F10 cells and use to study the intracellular fate of HPMA copolymer-doxorubicin. *J. Drug Targeting 14*, 375−390.
(26) Yang, Y., Sunoqrot, S., Stowell, C., Ji, J. L., Lee, C. W., Kim, J. W., Khan, S. A., and Hong, S. (2012) Effect of size, surface charge, and hydrophobicity of poly(amidoamine) dendrimers on their skin penetration. *Biomacromolecules 13*, 2154−2162.
(27) Perumal, O. P., Inapagolla, R., Kannan, S., and Kannan, R. M. (2008) The effect of surface functionality on cellular trafficking of dendrimers. *Biomaterials 29*, 3469−3476.
(28) van Dongen, M. A., Desai, A., Orr, B. G., Baker, J. R., and Holl, M. M. B. (2013) Quantitative analysis of generation and branch defects in G5 poly(amidoamine) dendrimer. *Polymer 54*, 4126−4133.
(29) Mullen, D. G., Borgmeier, E. L., Desai, A. M., van Dongen, M. A., Barash, M., Cheng, X. M., Baker, J. R., and Holl, M. M. B. (2010) Isolation and characterization of dendrimers with precise numbers of functional groups. *Chem.—Eur. J. 16*, 10675−10678.
(30) Selwyn, J. E., and Steinfeld, J. I. (1972) Aggregation equilibria of xanthene dyes. *J. Phys. Chem. 76*, 762−774.
(31) van Dongen, M., Orr, B. G., and Banaszak Holl, M. M. (2014) Diffusion NMR study of generation five PAMAM dendrimer materials. *J. Phys. Chem. B 118*, 7195−7202.
(32) Chen, L. C., Lloyd, W. R., Chang, C. W., Sud, D., and Mycek, M. A. (2013) Fluorescence lifetime imaging microscopy for quantitative biological imaging. *Methods Cell Biol. 114*, 457−488.
(33) Lin, H.-J., Herman, P., and Lakowicz, J. R. (2003) Fluorescence lifetime-resolved pH imaging of living cells. *Cytometry, Part A 52A*, 77−89.
(34) Unruh, J. R., Gokulrangan, G., Wilson, G. S., and Johnson, C. K. (2005) Fluoresence properties of fluorescein, tetramethylrhodamine and texas red linked to a DNA aptamer. *Photochem. Photobiol. 81*, 682−690.

DOI: 10.1021/bc5005735
Bioconjugate Chem. 2015, 26, 304−315

(35) Thomas, T. P., Majoros, I., Kotlyar, A., Mullen, D., Holl, M. M. B., and Baker, J. R. (2009) Cationic poly(amidoamine) dendrimer induces lysosomal apoptotic pathway at therapeutically relevant concentrations. *Biomacromolecules 10*, 3207−3214.
(36) Xu, Z. J., He, B. C., Shen, J., Yang, W. T., and Yin, M. Z. (2013) Fluorescent water-soluble perylenediimide-cored cationic dendrimers: synthesis, optical properties, and cell uptake. *Chem. Commun. 49*, 3646−3648.
(37) Ornelas, C., Lodescar, R., Durandin, A., Canary, J. W., Pennell, R., Liebes, L. F., and Weck, M. (2011) Combining aminocyanine dyes with polyamide dendrons: a promising strategy for imaging in the near-infrared region. *Chem.—Eur. J. 17*, 3619−3629.
(38) Ornelas, C., Pennell, R., Liebes, L. F., and Weck, M. (2011) Construction of a well-defined multifunctional dendrimer for theranostics. *Org. Lett. 13*, 976−979.
(39) Vámosi, G., Gohlke, C., and Clegg, R. M. (1996) Fluorescence characteristics of 5-carboxytetramethylrhodamine linked covalently to the 5′ end of oligonucelotides: multiple conformers of single-stranded and double-stranded dye-DNA oligomers. *Biophys. J. 71*, 972−994.
(40) Rattan, R., Vaidyanathan, S., Wu, G. S. H., Shakya, A., Orr, B. G., and Holl, M. M. B. (2013) Polyplex-induced cytosolic nuclease activation leads to differential transgene expression. *Mol. Pharmaceutics 10*, 3013−3022.

DOI: 10.1021/bc5005735
Bioconjugate Chem. 2015, 26, 304−315